

A magneto-reflectivity study of CuGaSe₂ single crystals

Michael V. Yakushev,^{1,2,3,4*} Alexander V. Mudryi,⁵ Clement Faugeras⁶
and Robert W. Martin²

¹ M.N. Miheev Institute of Metal Physics of the UB RAS, 18 S. Kovalevskoy St. 620108, Ekaterinburg, Russia.

² Department of Physics, SUPA, Strathclyde University, G4 0NG Glasgow, UK.

³ Ural Federal University, 19 Mira St., 620002 Ekaterinburg, Russia.

⁴ Institute of Solid State Chemistry of the Urals branch of the Russian Academy of Sciences, Ekaterinburg, 620990, Russia.

⁵ Scientific-Practical Material Research Centre of the National Academy of Belarus, 19 P. Brovki, 220072 Minsk, Belarus.

⁶ LNCMI-CNRS (UJF, UPS, INSA), BP 166, 38042 Grenoble Cedex 9, France.

Keywords CuGaSe₂, Excitons, Magnetic field.

* Corresponding author: e-mail michael.yakushev@strath.ac.uk

CuGaSe₂ single crystals were studied using magneto-reflectivity at 4.2 K in magnetic fields B up to 20 T. The A and B free excitons, observed in the optical reflectivity spectra, blue shift with increasing B . A low-field perturbation approach within the hydrogenic model is used to fit the dependence of the spectral position of these excitons on B . The A and B exciton reduced masses of $0.115m_0$ and $0.108m_0$ (m_0 is the free electron mass), Rydbergs of 12.9 meV and 12.2 meV, Bohr radii 5.08 nm and 5.4 nm, and effective hole masses of $0.64m_0$ and $0.48m_0$, respectively, are determined.

1 Introduction CuGaSe₂ is a technologically important semiconductor compound used in the absorber layer of solar cells with a record conversion efficiency of 22.6% [1]. In such cells CuGaSe₂ is alloyed with CuInSe₂ to tune the band gap E_g of the absorber layers close to the optimal range for solar energy conversion. In terms of efficiency the CuInGaSe₂-based photovoltaic (PV) devices are amongst leading thin film technologies [2].

However the achieved efficiency records for CuInGaSe₂-based PV is still lower than a one-junction solar cell theoretical limit of 30% [3] suggesting a lack of knowledge on the fundamental electronic properties of CuInGaSe₂ in general and CuGaSe₂ in particular where some parameters of the electron structure are still known only from theoretical studies [4]. To become reliable theoretically determined parameters should also be verified by experiment.

The difference in the Cu-Se and Ga-Se bonding in the chalcopyrite structure of CuGaSe₂ induces a tetragonal distortion splitting the valence band into the A, B and C sub-bands [5]. In terms of the quasi-cubic model [6] such a distortion is considered to be a result of the non-cubic crystal field along with the spin-orbital interaction splitting the otherwise triply degenerated valence band into three sub-bands.

The charge carrier effective masses affect the transport properties of semiconductor devices determining the mobility which is of a direct importance for solar cell technology development. Such masses can be measured experimentally from magneto-optical spectra of free excitons, comprising electrons from the conduction band and holes from the valence band, under the influence of magnetic fields [7-9]. Increasing magnetic fields blue shift the energy level of these excitons. The rate of such shifts reflects the confinement degree of the excitons and can be used to determine their Bohr radii and reduced masses [11-12]. Magneto-optical measurements have been used to determine exciton reduced masses and Bohr radii

separately for the A, B and C excitons in CuInSe₂ [9,10,13] as well as the A and BC excitons in CuInS₂ [8] providing an opportunity to determine hole masses corresponding to these sub-bands. For CuGaSe₂ only the A exciton shifts in magnetic fields have been examined by magneto-photoluminescence [7] (MPL) whereas shifts of both the A and B excitons can be examined simultaneously analysing magneto-reflectivity spectra which provides a chance to determine the A and B-hole masses. The B-hole mass in CuGaSe₂ has been determined only theoretically [4]. Mass values of this hole are important for the development of the kp theory for the chalcopyrites.

In this letter we present a study of the effect of magnetic fields on the optical reflectivity (OR) spectra of CuGaSe₂ single crystals used to determine the reduced mass and Bohr radius of the A and B free excitons as well as the effective hole mass for these sub-bands.

2 Experimental methods Single crystals of CuGaSe₂ were grown by the vertical Bridgman technique [14] assuming a melting point of 1050 °C from pseudo-binary phase diagram reported in ref. [15]. Although, according to this diagram, CuGaSe₂ is formed by a peritectic solidification, excitonic quality crystals can be grown from the melt of a near stoichiometric mix of high purity Cu, Ga and Se at slow cooling rates [16]. X-ray diffraction patterns demonstrated no secondary phases in the material.

Freshly cleaved surfaces of these samples were at first examined at 4.2 K by photoluminescence (PL) and OR at zero magnetic fields. The samples then were introduced into the bore of a 10 MW resistive magnet (providing magnetic fields B up to 20 T) in the Faraday configuration: the examined sample surface being perpendicular to the magnetic field direction and the direction of the excitation light. The magneto-reflectance (MR) measurements were carried out in the Grenoble High Magnetic Field Laboratory. The 514

nm line of an argon ion laser was used to excite PL emission whereas a halogen tungsten lamp was used for the MR measurements. Optical fibres were employed to transmit the excitation laser- and lamp-beam to the sample surface and to collect PL and MR signals as well as to deliver these signals to the slits of a 0.5 m spectrometer with 1800 grooves/mm grating blazed at 500 nm. These fibres were not polarisation maintaining ones. The dispersed signal was detected by a liquid nitrogen cooled silicon CCD. The measurements were carried out with a spectral resolution of 0.2 meV. The orientation of the lattice structure of the measured crystals with respect to the magnetic field direction was not examined. More details about the experimental set up can be found elsewhere [7-10].

3 Results and discussions The excitonic region of the OR and PL spectra of the analysed CuGaSe₂ samples, measured at 4.2 K, is shown in Fig. 1(a) and (b), respectively. The OR spectrum demonstrates a sharp excitonic resonance at 1.728 eV and a more rounded one at 1.809 eV. These resonances have earlier been assigned to the A and B free excitons [17]. A sharp peak of the A exciton can also be seen in the PL spectrum, shown in Fig. 1(b). The full width at half maximum (FWHM) of this peak is of 3.2 meV suggesting a high structural quality of the material. The second peak in the PL spectrum at 1.724 eV has been assigned to exciton bound to a neutral acceptor (BE) [18]. In this report we concentrate our attention on the effect of magnetic fields on the free A and B excitons in the MR spectra. The evolution of these spectra under the influence of magnetic fields, shown in Fig.2, demonstrates how magnetic fields B blue shift both excitonic resonances.

To improve the accuracy of determining the exciton spectral position the reflectivity spectra were fitted with the following function [19]:

$$R(E) = R_0 + R_x \operatorname{Re} \left\{ e^{i\theta} (E_x - E + i\Gamma_x) / [\Gamma_x^2 + (E_x - E)^2] \right\}, \quad (1)$$

where E_x is the spectral energy of the A or B excitons, Γ_x is the broadening parameter of these excitons and θ is a phase ($\theta_A = \theta_B$) and R_x is an amplitude, R_0 is a background.

Lorentz forces in magnetic fields deform the relative motion of the electron and hole in the exciton [11]. At weak magnetic fields, such a deformation does not break the Coulomb forces between the hole and electron and can be treated as a perturbation admixing the p -type envelope wave-functions with the angular momentum $l = 1$ to the originally s -type function of the exciton ground state ($l = 0$). The angular momentum thus becomes proportional to the strength of magnetic field B . In magnetic fields the magnetic dipole energy is also proportional to B . Therefore in weak magnetic

fields the difference between the exciton energy at field B $E(B)$ and its zero-field energy $E(0T)$ quadratically depends on B [11]:

$$E(B) - E(0T) = \Delta E_d(B) = c_d B^2, \quad (2)$$

where c_d is a diamagnetic coefficient representing the rate of the shift. This rate is proportional to the square size of the exciton wave-function in the plane perpendicular to B .

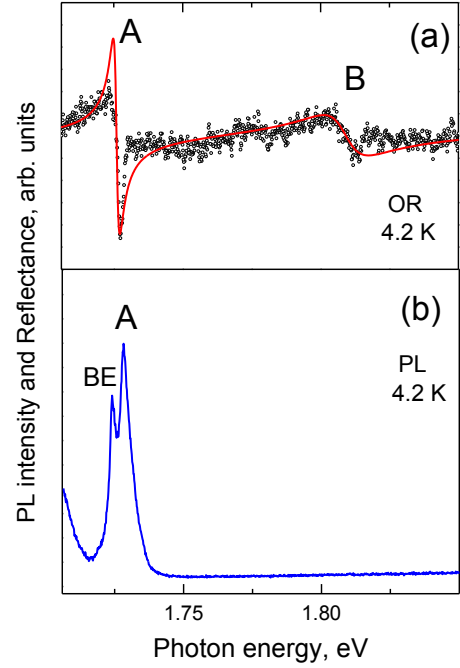


Figure 1 Zero field (a) OR spectrum (\circ) with A and B excitons, red line is the best fit, (b) PL spectrum with A free and BX bound excitons.

The dependence of the spectral position of the A and B excitons on B is shown in Fig. 3. Quadratic functions (2) were fitted to the experimental points gradually increasing the number of experimental points (and consequently the upper limit of B) from 4 to 20 T. The correlation coefficients R^2 , reflecting the quality of the fit, at first increased with rising number of the points until 9 T for the B exciton and 13 T for the A exciton. Further increases in the point number resulted in a reduction of R^2 . The best fits, corresponding to the maximum R^2 are shown in Fig.3. These fits correspond to diamagnetic shift rates c_d of $(0.985 \pm 0.02) \times 10^{-5}$ eV/T² for the A and $(1.17 \pm 0.02) \times 10^{-5}$ eV/T² for the B excitons. It can be seen that the quadratic functions at B in excess of 13 T and 9 T (for the A and B excitons, respectively) become greater than the experimental points indicating the limits of B after which the weak field model stops working [20].

Perturbation theories, developed for Wannier excitons, neglect the interaction of the A and B valence sub-bands [12, 21]. For an isotropic hydrogenic 1s exciton the first order perturbation solution of the exciton Hamiltonian in magnetic fields results for both theories in a similar diamagnetic term relating the energy shift ΔE_d to the Bohr radius a_B as follows:

$$\Delta E_d = (e^2 a_B^2 / 4\mu) B^2 = (4\pi^2 \hbar^4 \varepsilon^2 \varepsilon_0^2 / e^2 \mu^3) B^2, \quad (3)$$

where ε and ε_0 are the static dielectric constant and the permittivity in vacuum, respectively, whereas $\mu = (1/m_e + 1/m_h)^{-1}$ is the exciton reduced mass combining the electron m_e and hole m_h masses.

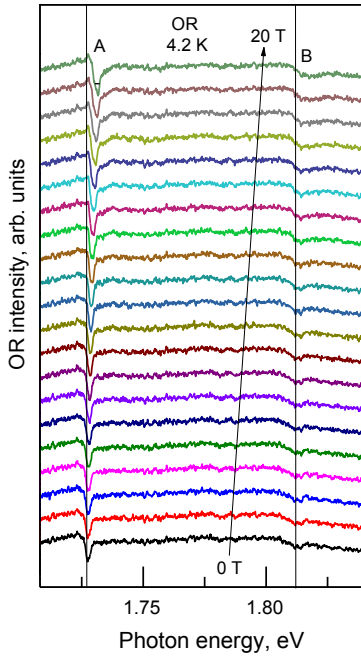


Figure 2 The effect of the magnetic field B , increasing from 0 T to 20 T, on the MR spectra of the free A and B exciton.

Assuming a theoretical dielectric constant of $\varepsilon = 10.6$ [4], which is the average of slightly anisotropic values of ε along and perpendicular to the tetragonal axis in CuGaSe₂, and using equation (3) we determine the reduced masses of the A and B excitons $\mu_A = 0.115m_0$ and $\mu_B = 0.108m_0$, respectively, where m_0 is the free electron mass. These hole masses are also collected in Table 1.

To find the effective electron mass we used the theoretically predicted dependence of m_e in CuIn_{1-x}Ga_xSe₂ on the Ga content x : $m_e(\text{CuIn}_{1-x}\text{Ga}_x\text{Se}_2) = [m_e(\text{CuInSe}_2) + 0.05x]m_0$. For the electron effective mass in CuInSe₂ we used the experimental value of $m_e(\text{CuInSe}_2) = 0.09m_0$ [22] resulting in $m_e(\text{CuGaSe}_2) = 0.14m_0$. Using this m_e we calculated the A valence sub-band hole mass $m_h(\text{A}) = 0.64m_0$ and B

valence sub-band hole mass $m_h(\text{B}) = 0.48m_0$. Both values can also be found in Table 1. Significant differences of the hole masses, theoretically calculated in ref. [4] and those experimentally measured in CuInGaSe₂ using optical spectroscopy, are attributed to the strong non-parabolicity of the valence band in these materials.

The determined A hole mass has the same value as the one determined earlier using weak field MPL measurements [7]. Our experimental hole masses are significantly greater than the density of state hole masses of $0.32m_0$ and $0.29m_0$ theoretically determined for the A and B holes, respectively [4].

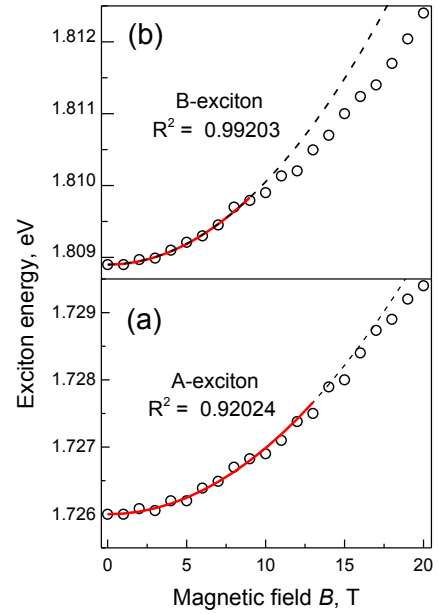


Figure 3 The experimental dependencies of the A (a) and B (b) exciton spectral position on the increasing magnetic fields (○). The solid lines are best fits using quadratic functions.

The hole masses, experimental determined using magneto-optics for CuInSe₂ [13], are also greater than those from theoretical studies which has been explained by non-parabolicity of the valence band [4]. The A and B excitonic Rydbergs of 12.9 meV and 12.2 meV, respectively, were calculated, using the following expression [11]:

$$Ry^* = \mu / (m_0 \varepsilon^2) Ry \quad (4)$$

where $Ry = 13.6$ eV is the Rydberg constant. The A exciton effective Rydberg Ry^* is very close to the A exciton binding energy 13 ± 2 meV, determined from the experimentally measured spectral energy of the A exciton first excited state [18]. The Bohr exciton radii of are estimated to be $a_B(\text{A}) = 5.1$ nm and $a_B(\text{B}) = 5.4$. The determined values are also shown in Table 1.

The diamagnetic shift rate of 0.98×10^{-5} eV/T² for the A exciton in CuGaSe₂ [7], measured using MPL, is in good agreement with our results. The smaller c_d for the B exciton in our study can be attributed to the smaller B-hole mass in comparison with the A-hole mass $m_h(A) = 0.64m_0$ in the A exciton.

In CuInSe₂ the diamagnetic shift rate, averaging c_d for the magnetic field \mathbf{B} along and perpendicular to the tetragonal direction of the CuInSe₂ lattice, were reported as 2.82×10^{-5} eV/T² and 2.35×10^{-5} eV/T² [13], for the A and B excitons, respectively, also found for the weak magnetic fields, are significantly greater than that in CuGaSe₂. This can be attributed to the larger Bohr radii of 9.5 nm and 9.9 nm for the A and B exciton, respectively, in CuInSe₂. On the other hand the diamagnetic shift rate of $4.5 \cdot 10^{-6}$ eV/T² and $4.5 \cdot 10^{-6}$ eV/T², for the A and BC free exciton lines in CuInS₂, respectively, are significantly smaller than those determined in this study. These differences are consistent with smaller excitonic Bohr radii of 3.8 nm and 3.8 nm, respectively, in CuInS₂.

Table 1 Diamagnetic shifts c_d , reduced masses μ , effective Rydbergs (Ry^*), Bohr radii (a_B) of the A and B free excitons and their effective hole masses, m_h .

Exciton	c_d (eV/T ²)	μ/m_0	Ry^* (meV)	a_B (nm)	m_h/m_0
A	0.985×10^{-5}	0.115	12.9	5.1	0.64
B	1.17×10^{-5}	0.108	12.2	5.4	0.48

4 Conclusion Diamagnetic shift rates of 0.985×10^{-5} eV/T² and 1.17×10^{-5} eV/T² were measured for the A and B free exciton, respectively, from magneto-reflectivity spectra of CuGaSe₂ single crystals. These rates were used to calculate the A and B exciton reduced masses ($0.115m_0$ and $0.105m_0$), their Rydbergs (12.9 meV and 12.2 meV), Bohr radii (5.1 nm and 5.4 nm) as well as the effective hole masses ($0.64m_0$ and $0.42 m_0$) using a first-order perturbation model within the hydrogenic model of free exciton.

Acknowledgements The crystal growth was supported by the FASO of Russia (“Quantum” № 01201463332), the magneto-optical study was supported by the Russian Science Foundation (grant 17-12-01500) and LNCMI-CNRS (EMFL).

References

- [1] P. Jackson, R. Wuerz, D. Hariskos, E. Lotter, W. Witte, M. Powalla. Phys. Status Solidi RRL, **10**, 583 (2016).
- [2] M.A. Green, Y. Hishikawa, E.D. Dunlop, D.H. Levi, J. Hohl-Ebinger, A.W.Y. Ho-Baillie. Prog. Photovolt. Res. Appl., **26**, 3 (2018).
- [3] W. Shockley, H.J. Queisser. J. Appl. Phys., **32**, 510 (1961).
- [4] C. Persson, Appl. Phys. Lett. **93**, 072106 (2008).

- [5] J. L. Shay, & J. H. Wernick, *Ternary Chalcopyrite Semiconductors-Growth, Electronic Properties, and Applications*. (Pergamon, 1975).
- [6] J. E. Rowe and J. L. Shay, Phys. Rev. B **3**, 451(1976).
- [7] F. Luckert, M. V. Yakushev, C. Faugeras, A. V. Karotki, A. V. Mudryi, and R. W. Martin, Appl. Phys. Lett. **97**, 162101 (2010).
- [8] M.V. Yakushev, R.W. Martin and A.V. Mudryi, Appl. Phys. Lett. **94** (2009) 042109.
- [9] M.V. Yakushev, R.W.Martin, A. Babinski and A.V. Mudryi, Physica Status Solidi (c) **6**, 1086 (2009).
- [10] M.V. Yakushev, F. Luckert, A.V. Rodina, C.Faugeras, A.V. Mudryi, A.V.Karotki and R.W. Martin, Appl. Phys. Lett. **101**, 262101 (2012).
- [11] C.F. Klingshim, *Semiconductor Optics*. (Springer-Verlag, 1995).
- [12] S. Taguchi, T. Goto, M. Takeda, G. Kido, Phys. Soc. Jpn. **57**, 3256 (1988).
- [13] M.V. Yakushev, A.V. Rodina, G.M. Shuchalin, R.P. Seisian, M.A. Abdullaev, A. Rockett, V.D. Zhivulko, A.V. Mudryi, C. Faugeras, and R.W. Martin, Appl. Phys. Lett. **105**, 142103 (2014).
- [14] R.D. Tomlinson, Solar cells, **16**, 17 (1986).
- [15] L.S. Palatnik and E.K. Belova, Izv. Akad. Nauk SSSR, Neorgan. Mater.**3**, 967 (1967).
- [16] A.V. Mudryi, I.V. Bodnar, V.F. Gremenok, I.A. Victorov, A.I. Patuk, I.A. Shakin, Solar Energy Materials and Solar Cells **53**, 247 (1998).
- [17] B. Tell, P. M. Bridenbanch. Phys. Rev. B. **12**, 3330 (1975).
- [18] A. Bauknecht, S. Siebentritt, J. Albert, Y. Tamm, M. Ch. Lux-Steiner, Jpn. J. Appl. Phys. **39** (Suppl. 39-1), 322 (2000).
- [19] K.P. Korona, A. Wyszomolek, K. Pakula, R. Stepniewski, J. M. Baranowski, I. Grzegory, B. Lucznik, M. Wroblewski, and S. Porowski, Appl. Phys. Lett. **69**, 788 (1996).
- [20] P.C. Makado and N. C. McGill, Journal of Physics C-Solid State Physics **19**, 873 (1986).
- [21] R. G. Wheeler and J. O. Dimmock, Phys. Rev. **125**, 1805(1962).
- [22] H. Weinert, H. Neumann, H. J. Hobler, G. Kuhn, N. V. Nam, Phys. Stat. Sol. B **81**, K29 (1977).